

# Application of Dual-Doped TMAH Silicon Etchant in the Fabrication of a Micromachined Aluminum Flexing Beam Actuator

John Garra, Sebastiano Brida<sup>1</sup>, Lorenza Ferrario<sup>1</sup> and Makarand Paranjape\*

Department of Physics, Georgetown University, Washington, D.C. 20057, USA

<sup>1</sup>Istituto per la Ricerca Scientifica e Tecnologica (ITC-Irst), Trento, ITALY

(Received September 1, 2000; accepted December 1, 2000)

**Key words:** TMAH with additives, aluminum actuator, CMOS-compatible, magnetometer

One of the main goals of microelectromechanical system (MEMS) fabrication is micro-device integration with standard integrated circuit (IC) technologies, such as bipolar or the more prevalent complementary metal oxide semiconductor (CMOS) processes. To that end, it has been found that the anisotropic silicon etchant tetra-methyl ammonium-hydroxide (TMAH) can be effectively used in a post-processing step with CMOS-based fabrication by doping it with silicic acid to prevent the unwanted etching of exposed aluminum. Furthermore, the addition of ammonium persulfate to the TMAH/silicic acid solution enhances etch rate and surface quality. The final etching solution, called dual-doped TMAH, is CMOS-compatible, highly selective to silicon over aluminum, and can therefore allow an aluminum layer to be used as an etch mask. In this paper, we utilize dual-doped TMAH towards the fabrication of a microstructure made entirely of aluminum. A flexing beam microactuator suspended over a bulk micromachined silicon cavity is presented for use as a magnetometer.

## 1. Introduction

Microelectromechanical systems (MEMS) are often fabricated of silicon because many of the process techniques are fundamentally the same as those used in standard integrated circuit (IC) fabrication. MEMS fabrication often requires an anisotropic silicon etchant to create deep, well-defined grooves, cavities, or suspended structures. The quaternary

---

\*Corresponding author

ammonium-based alkaline solution, tetra-methyl ammonium hydroxide, or TMAH, is a silicon etchant that is finding greater use because of its high etch rate, selectivity to silicon over common dielectric masking layers such as silicon oxide and silicon nitride, anisotropy, and low toxicity.

Two problems are normally associated with the use of TMAH in the fabrication of MEMS devices. First, TMAH etches aluminum very rapidly. This is problematic because one of the main goals of MEMS design is the integration of control electronics (generally complementary metal-oxide semiconductor, or CMOS) with the microdevice. Given that any exposed aluminum is attacked by TMAH, co-integration of MEMS with CMOS is not a compatible post-processing step in light of the exposed aluminum bonding pads. The second problem is a characteristic drop off in the silicon etch rate over time for low-concentration TMAH. The reduction in etch rate is caused by the formation of tiny protrusions called "hillocks" on the  $\langle 100 \rangle$  silicon surface.<sup>(1-5)</sup> Hillock formation is normally suppressed in higher concentration solutions, but the etch rate is intrinsically lower.

It has been found that both problems can be alleviated simultaneously by doping TMAH with silicic acid  $[\text{H}_4\text{SiO}_4]$ <sup>(6)</sup> (SA) and ammonium persulfate (AP).<sup>(7-9)</sup> The effect of each additive is described in Section 2. The improved low-concentration solution, or dual-doped TMAH, has been shown to have characteristics similar to those of better-behaved high concentration TMAH solutions, with the added benefits of an increased, constant silicon etch rate and selectivity over aluminum.<sup>(6)</sup> In this paper, the role of dual-doped TMAH will be explained in the fabrication of an aluminum microstructure — a micromachined flexing beam actuator for sensing and measuring magnetic fields. The device is comprised of an aluminum beam suspended over a silicon etch cavity and held by four support arms, each connected to a rectangular bonding pad on the unetched silicon substrate. The support arms are attached to the sides of the beam at the nodal points of its fundamental mode of vibration, as determined by mechanical simulation. The bonding pads firmly anchor the device and provide contact points for applying an AC bias across the midspan of the beam. The device is to be driven by an alternating current with a frequency equal to the mechanical resonant frequency of the aluminum beam. In the presence of a magnetic field in the plane of the beam and perpendicular to its major length, a Lorentz force acts on the charge carriers, deflecting them either upward or downward. These deflections are translated to the beam, and its amplitude of vibration is proportional to both the strength of the magnetic field and the magnitude of the drive current.<sup>(10)</sup> Several methods for detecting the vibration of the beam are being considered.

## 2. Dual-Doped TMAH

The silicon etch rate of undoped TMAH increases with temperature and reduced solution concentration.<sup>(6)</sup> However, a major drawback for low-concentration solutions is the formation of hillocks on the  $\langle 100 \rangle$  surface. The sides of the hillocks all lie on near- $\langle 111 \rangle$  crystal planes, which etch extremely slowly in TMAH. Hillocks are formed through the micromasking effect of bubbles that form and stick to the silicon etch front

during etching. Bubble formation is greatest for low-concentration TMAH solutions, which have a low pH. It is presumed that a polymer masking layer forms beneath the bubble and disrupts the otherwise smooth and uniform etching of the <100> surface. If the entire silicon surface becomes covered by hillocks, the etch rate is significantly reduced to a near-zero value.<sup>(6)</sup> With many bulk micromachining applications, there is often a need to etch through most of the thickness of the wafer in a timely manner (*e.g.*, to create a thin sensing membrane). Suppression of hillocks is generally guaranteed for high concentrations of TMAH, but the intrinsic etch rate at these concentrations is somewhat low, requiring very long etch times for through-wafer etching applications. Therefore, use of TMAH at lower concentrations has the advantage of being more economical in terms of cost and time, but only if the hillock problem can be eliminated.

Ammonium persulfate (AP) is an oxidizer that is used to control the problem of hillock formation in low-concentration TMAH.<sup>(1,7,8)</sup> When AP is added to low-concentration TMAH at preset intervals (to prevent depletion of the oxidizer during the etching process), few to no hillocks are formed and a high, constant etch rate is achieved.<sup>(6)</sup> AP appears to reduce the size of the bubbles formed, thereby reducing their dwell time, or the time the bubbles reside on the silicon surface producing micromasking effects.

The TMAH/AP solution still etches aluminum vigorously, but the etch selectivity to silicon over aluminum can be improved by additionally doping the solution with silicic acid. The presence of silicates in the solution causes the formation of an aluminosilicate passivation layer on the exposed aluminum. Aluminosilicates are less soluble at moderate pH levels than the hydrated aluminum oxide that would normally form in an undoped solution. The acid also decreases the pH level of the solution, increasing the longevity of the aluminosilicate passivation layer. Normally, the reduced pH level caused by the addition of silicic acid would be conducive to hillock formation. However, with our dual-doped etchant, hillock formation is blocked by the presence of ammonium persulfate in solution. The result is a silicon etchant comparable to undoped, high-concentration TMAH in terms of anisotropy, dielectric mask selectivity, and surface quality. More importantly, the low-concentration dual-doped TMAH possesses a high selectivity over aluminum and has an enhanced etch rate.

### 3. Fabrication

#### 3.1 Initial experiment

Aluminum was chosen for the structural material of the flexing beam magnetometer because of its availability and its low as-deposited intrinsic stress. Unlike oxides, deposited aluminum is relatively stress-free, making it a good material for creating suspended structures.

After an initial wet oxidation to produce a 380-nm-thick oxide masking layer, a 700-nm-thick aluminum structural layer was evaporated over the entire <100> silicon wafer. The aluminum was then patterned to create the main device structure. Next, the oxide layer was patterned using an etchant with high selectivity to oxide over aluminum in order to allow etching of a silicon cavity beneath the beam. The device layout, dimensions, and the configuration of the layers are illustrated in Fig. 1. (There were also some variations on this

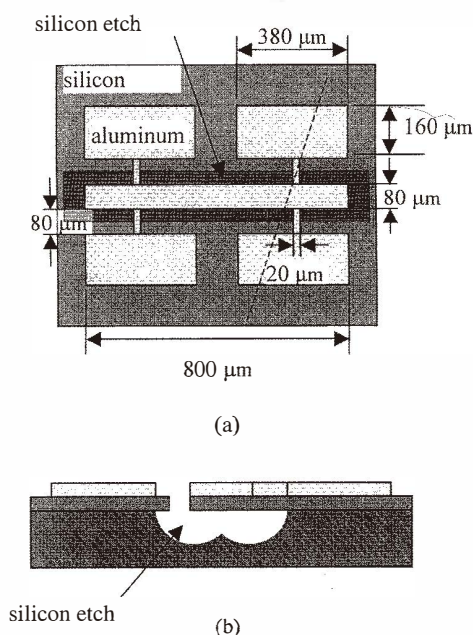


Fig. 1. Illustration of device layout. (a) Top view shows shape of aluminum structure and location of silicon cavity beneath beam. (b) Cross section taken along the dashed line in part (a) shows aluminum beam on top of oxide masking layer.

design as explained in Section. 3.4). Only two masks are required in the fabrication process: an aluminum etch mask and an oxide etch mask. The masks were printed onto linotronic film by a desktop publishing service, which offered a resolution limit of approximately  $20\ \mu\text{m}$ . The patterns on the films were then transferred to conventional iron oxide mask plates using photolithography.

The layout of the device was made parallel to the  $\langle 110 \rangle$  primary flat since, originally, the silicon cavity was to be etched with xenon difluoride ( $\text{XeF}_2$ ). Xenon difluoride is a gas phase, isotropic silicon etchant and was chosen because of its high etch selectivity of silicon over aluminum. The etching is carried out in pulses as the  $\text{XeF}_2$  gas is pumped into a small vacuum chamber, left to etch the silicon for about one minute, and then pumped out before adding another dose. It is estimated that the silicon etch rate is approximately one micron per minute. The progress during the etching process can be monitored visually through a microscope or video unit.

### 3.2 Initial results

The isotropic silicon etch required close monitoring because the  $\text{XeF}_2$  could undercut the bonding pads as well as the beam if it were allowed to proceed for too long. The device dimensions were planned so that the beam could be completely undercut before the etchant

began to remove the silicon beneath the pads. However, performing such a precise etch with an isotropic etchant is not easy. For most of the devices in our sample, the progress of the lateral etch front was underestimated and many of the beams remained unreleased, bonded to the silicon substrate. One of the reasons for the lack of etch precision was the roughness of the etch front and of the etched surface.

Another problem encountered with this design was that the oxide layer remaining on the underside of the beam transferred its stress to the aluminum, causing the ends of the beam to curl up severely upon release from the substrate. Although it was thought that removing the oxide as the final step could straighten the curled beams, this proved incorrect as the aluminum had been irreversibly deformed.

### 3.3 Improved design

An etchant with a higher degree of precision would be required to release the beam without undercutting the bonding pads. Dual-doped TMAH provided a partial solution to the problem. Its anisotropy would allow for a precise, well-defined etch cavity while its selectivity to silicon over aluminum would ensure that the aluminum structure would not be destroyed during the etching process. However, the device had been designed to be etched isotropically, and it was apparent that no anisotropic etchant could undercut the center section of the beam because it would be stopped by the  $\langle 111 \rangle$  crystal planes aligned with the sides of the beam. Therefore, the first step was to make an initial etch into the silicon cavity using a relatively isotropic reactive ion etching (RIE) process. The goal of the reactive ion etching was to produce shallow ( $\sim 10 \mu\text{m}$ ) trenches in the exposed silicon. Due to the isotropy of the RIE recipe, a  $10\text{-}\mu\text{m}$ -deep etch was sufficient to laterally undercut the  $20\text{-}\mu\text{m}$ -wide support arms, thereby allowing the subsequent TMAH etch to release the beam. The dual-doped TMAH used for the silicon etch comprised 190 ml of 6.25% wt. TMAH, 7.8 g of silicic acid, and 10 ml of a 200 ml stock solution of 40 g ammonium persulfate dissolved in 200 ml of 6.25% wt. TMAH.

In addition, to alleviate the beam curling problem mentioned earlier, the oxide masking layer was patterned prior to deposition of the aluminum. This sequence change placed the beam in direct contact with the underlying silicon, which would later be etched away (see Fig. 2). The curl-inducing oxide layer was eliminated. Additionally, the thickness of the aluminum layer was increased to  $2 \mu\text{m}$  to increase the rigidity of the beam and to further reduce the possibility of curling.

### 3.4 Final outcome

An intermediate step revealed that the patterned oxide masking layer, required to create the etch cavity beneath the beam, was destroyed during the isotropic RIE. The etch ratio of



Fig. 2. Cross section of the improved design. The oxide layer beneath the beam has been removed and the silicon cavity has been etched anisotropically. Compare with Fig. 1(b).

silicon to oxide with this RIE recipe is only 10 at best (the etch ratio of silicon to aluminum is very high). It was necessary to increase the thickness of the oxide film from 180 nm to 600 nm in order for it to survive the RIE process.

The combination of an initial RIE followed by an etch with dual-doped TMAH created a precisely defined cavity beneath the beam. This cavity is visible in the SEM micrograph in Fig. 3.

Some beams were more responsive to the combined etching process than others as a result of the intended variation in their design. The purpose of varying the design was to produce a range of devices with the expectation that some might perform better than others. The beam widths were 50  $\mu\text{m}$ , 80  $\mu\text{m}$ , 120  $\mu\text{m}$ , and 160  $\mu\text{m}$ , and each of the four was designed with and without holes through the surface. The purpose of the holes was to prevent any air damping effect on the beam's vibrations. The holes, as later predicted, also facilitated the complete undercutting of the beam by the combination etch process. Of the eight designs, only five were realized through fabrication. The holes in the 50, 120, and 160  $\mu\text{m}$  wide beams did not show up because of the limited resolution of the masks. The larger holes in the 80- $\mu\text{m}$ -wide beam did show up however, and this beam design was undercut most reliably. The response of the beam to a magnetic field has been confirmed by placing the beam in a relatively weak magnetic field and applying a DC bias across it via two of the four bonding pads. Micrographs of the flexing beam (bending into cavity) are shown in Fig. 4. As the current across the beam increases from zero to 600 milliamps, the beam flexes either into or out of the cavity depending on the direction of the current. When the signal is shut off, the beam becomes flat again. Above 600 milliamps, the device fails because joule heating causes the current-carrying support arms to melt. An ANSYS computer simulation of the device has predicted the beam to have a resonant frequency of about 35 kHz, as indicated in Fig. 5. Further testing of the device is required to confirm this value and to characterize the beam's vibrational response to magnetic fields.

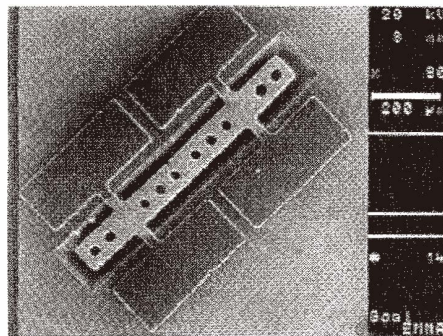


Fig. 3. SEM micrograph of the device shows the smooth etch cavity beneath the beam. The beam is 800  $\mu\text{m}$  long and 80  $\mu\text{m}$  wide.

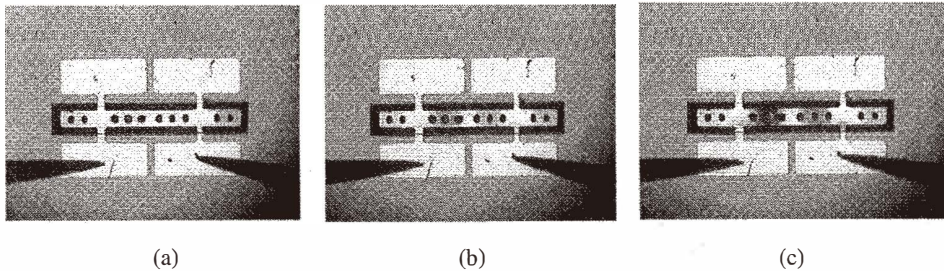


Fig. 4. Micrographs of the beam flexing in a magnetic field. A DC bias is applied across the device via the probes to produce a current of (a) 0 amps, (b) 300 mA and (c) 450 mA through the beam. The magnets generating the field are not visible here.

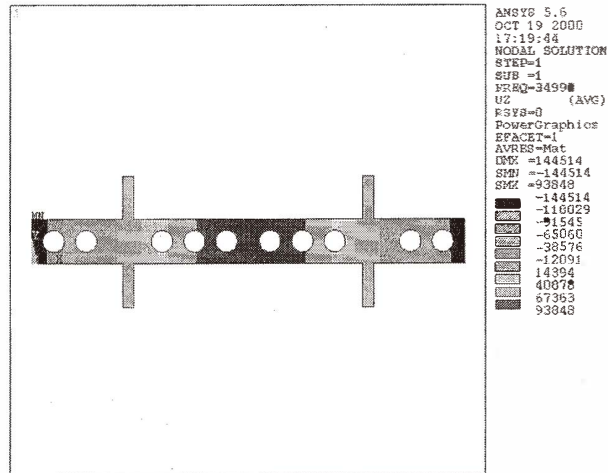


Fig. 5. Computer-generated ANSYS simulation of beam undergoing vibrations in its fundamental mode. Mechanical simulation predicts a resonant frequency of 34.99 kHz.

### 3.5 Future enhancements

First, the reason that reactive ion etching was necessary is that the device had been designed to be etched isotropically. RIE would not be required if the device were redesigned and oriented at an angle with respect to the  $\langle 100 \rangle$  crystal direction. This would allow dual-doped TMAH alone to create the silicon cavity because it would not encounter the  $\langle 111 \rangle$  crystal planes, thus eliminating a step from the fabrication process. Utilizing the full potential of TMAH's anisotropic properties would make complete undercutting of the beam more reliable and improve device yield.

Second, the desktop publishing service used to generate the masking patterns offered a limited resolution of 20  $\mu\text{m}$ . Masks with finer resolution would allow for narrower support

arms, increasing the flexibility of the beam and the sensitivity of the overall device. Finally, the addition of an interdigitated comb structure at the beam ends would allow for capacitive or interferometric detection methods.

#### **4. Conclusions**

TMAH is an anisotropic silicon etchant that is very useful in the fabrication of MEMS devices. Adding ammonium persulfate to low-concentration TMAH solutions prevents the formation of hillocks, which normally cause a significant reduction in etch rate. This AP + TMAH solution can be made compatible with CMOS fabrication by further adding silicic acid, which prevents aluminum etching and enables full MEMS device and electronics integration on a single silicon substrate. By using dual-doped TMAH, aluminum can be used as a non-conventional masking layer or as a structural material in a MEMS device such as the aluminum flexing beam actuator presented in this paper.

#### **Acknowledgements**

The authors would like to thank Don Novotny and Neil Green of the Georgetown Advanced Electronics Laboratory, and John Suehle of NIST for their assistance during fabrication. In addition, support from the Georgetown Undergraduate Research Opportunities Program is acknowledged by J. G.

#### **References**

- 1 U. Schnakenberg, W. Benecke and P. Lange: Proc. of the 6th Int'l Conf. on Solid-State Sensors and Actuators 1991 (Transducers '91) p. 815.
- 2 O. Tabata: *Sensors and Actuators A* **53** (1996) 335.
- 3 E. Klaassen, R. Reay, C. Storment, J. Audy, P. Henry, A. Brokaw and G.T.A. Kovacs: *Solid-State Sensor and Actuator Workshop* (Hilton, Head, SC 1996) p.127.
- 4 L. Landsberger, S. Naseh, M. Kahrizi and M. Paranjape: *J. of Microelectromechanical Sys.* **5** (1996) 106.
- 5 O. Tabata, R. Asahi, H. Funabashi and S. Sugiyama: Proc. of the 6th Int'l. Conf. on Solid-State Sensors and Actuators 1991 (Transducers '91) p. 811.
- 6 M. Paranjape, A. Pandey, S. Brida, L. Landsberger, M. Kahizi and M. Zen: *J. Vac. Sci. Technology A* **18** (2000) 738.
- 7 W. C. Erdman and P. F. Schmidt, US Pat. No. 3,738,881 (1973).
- 8 E. Klaassen, R. Reay and G. T. A. Kovacs: *Sensors and Actuators A* **52** (1996) 33.
- 9 M. Paranjape, S. Brida, V. Guarnieri, F. Giacomozzi and M. Zen: Proc. of the Can. Conf. on Elec. and Comp. Eng., 1999 (IEEE, Canada, 1999) p.1627.
- 10 R. B. Givens, J. C. Murphy, R. Osiander, T. J. Kistenmacher and D. K. Wickenden: *Appl. Phys. Lett.* **69** (1996) 2755.